

THE EFFECT OF ACRYLIC ACID AND ACRYLAMIDE GRAFT-COPOLYMERIZATION ON THE PROPERTIES OF SODIUM ALGINATE-BASED SUPERABSORBENT POLYMER

TZYY-JENG YONG¹, YAMUNA MUNUSAMY² & SWEE-YONG CHEE³

¹Faculty of Engineering and Green Technology, Universiti Tunku Abdul Rahman, Jalan Universiti, Bandar Barat,
Kampar, Perak, Malaysia

²Department of Petrochemical Engineering, Faculty of Engineering and Green Technology, Universiti Tunku Abdul
Rahman, Jalan Universiti, Bandar Barat Kampar, Perak, Malaysia

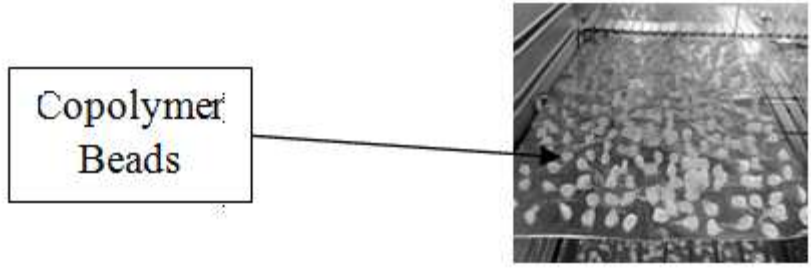
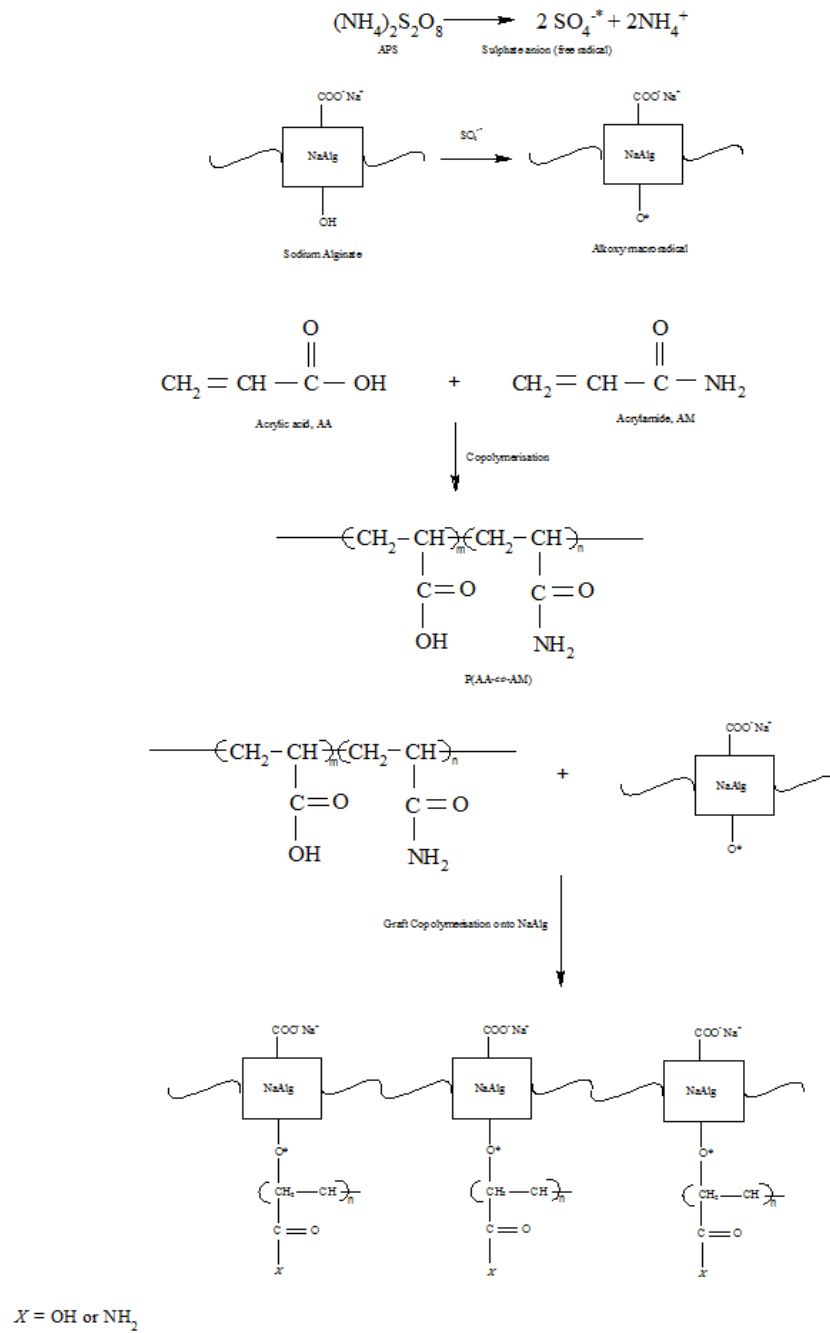
³Department of Chemical Science, Faculty of Science, Universiti Tunku Abdul Rahman, Jalan Universiti, Bandar Barat,
Kampar, Perak, Malaysia

ABSTRACT

Sodium alginate (NaAlg) copolymers were prepared by free radical grafting of acrylic acid (AA) and acrylamide (AM) onto NaAlg with the presence of ammonium persulfate (APS) initiator. The copolymers were then cross linked with N, N-methylenebisacrylamide (NMBA) to produce an interpenetrating network. The superabsorbent polymer (SAP) hydrogel was then dropped into Ca^{2+} solution to produce spherical copolymer beads. The main objective of the work is to study the effect of different ratio of AA and AM (85:15, 70:30, 55:45, 40:60 and 25:75) on the characteristic and performance of the SAP. Infrared (IR) spectroscopy proves successful grafting of AA and AM onto NaAlg backbone and formation of Ca^{2+} layer onto SAPs. Biodegradability and water absorbency decreases as AM concentration increases. Moreover, SEM study shows that the surface of copolymer beads with higher concentration of AM is compact with less cracks and pin holes. In addition, thermogravimetric analysis (TGA) and differential scanning calorimetry (DSC) also show that all the copolymer beads are thermally stable and the glass transition temperature (T_g) increases as AM concentration increases respectively.

KEYWORDS: Biodegradability Grafting Superabsorbent Swelling

Graphical Abstract



1. INTRODUCTION

Biodegradable superabsorbent polymers (SAPs) are cross-linked networks of hydrophilic polymers that can absorb, swell and retain a very large volume of water or other biological fluids and the fluid absorbed is hardly removable under pressure. Moreover, the macromolecules of these polymers are able to break down into smaller compounds or completely degrade in biologically active environment [1]. The biodegradation process is not only caused by microorganisms, but also through hydrolysis and oxidation process in biological environment [2].

Since the first superabsorbent polymer was reported by the US Department in Agriculture in 1961 [3], a lot of efforts have been attempted to modify their swelling capability [4-6], to improve their water absorbency, gel strength and absorption rate [7-9]. Due to the excellent properties relative to traditional water absorbing materials such as sponge, cotton and pulp, superabsorbent polymers are widely used in many fields such as hygienic products, horticulture, sealing, drug-delivery system and coal dewatering [10]. However, about 90% of traditional superabsorbent polymers are petroleum based, used in disposable articles and most of them are disposed in landfills or by incineration [11]. Thus, the incorporation of biodegradable and renewable natural high polyols, such as starch [12], cellulose [13] and chitosan [14], not only improve the biodegradability of superabsorbent polymers, but also can reduce the dependence on petrochemical-derived monomers.

Among all the polymers, alginic acid has gained immense popularity to be used as biodegradable superabsorbent polymer. It is a naturally occurring acidic polysaccharide extracted from the brown algae (*phylum phaeophyta*) and it exists as the most abundant polysaccharide in the brown algae, consisting of up to 40% of the dry matter [15]. Alginic acid is an unbranched block co-polymer consisting of two monosaccharide residues, (1,4)- β -D-mannuronic acid (M) and (1,4)- α -L-guluronic acid (G).

Alginic acid or sodium alginate has been widely used as additives in foods, traditional wound dressings, dental impression materials and pharmaceutical industry [16]. In this research, sodium alginate has been considered to be used for controlled release of fertilizer in plantations due to its strong water absorption and biodegradability.

Sodium alginate-based SAPs can be prepared by graft copolymerization of suitable vinyl monomers on alginate in the presence of a cross-linker. In this research, sodium alginate was graft copolymerized with AA and AM at different composition to produce a multifunctional biodegradable SAP. This multifunctional biodegradable SAPs have a large potential to be exploited to produce controlled release fertilizer. AA and AM monomers were chosen for the graft copolymerization due to their ionic and non-ionic nature respectively. This will lead to different characteristic of the SAP at different contact environment. To our knowledge no work has been done to graft AA and AM together in NaAlg backbone. Different concentration of AA and AM is expected to affect the water absorbency, thermal stability, crystallinity, surface morphology and biodegradability of the alginate based superabsorbent polymer.

2. EXPERIMENTAL

2.1. Materials

Pure Acrylic acid (AA) stabilized with 0.02% hydroquinone monomethylether and extra pure acrylamide (AM) were supplied by Sisco Research Laboratories Pvt. Ltd. (SRL). Sodium alginate (NaAlg) powder, ammonium persulfate (APS) initiator and calcium chloride solution with purity 99.5% were supplied by R&M Chemicals. N, N'-methylenebisacrylamide (NMBA) as crosslinker was supplied by Sigma-Aldrich.

2.2. Grafting of Sodium Alginate (NaAlg) with Acrylic Acid (AA) and Acrylamide (AM)

Sodium alginate copolymers with different ratio of AA and AM composition were prepared according to formulation in Table 1. The samples are designated as sample A, B, C, D and E.

NaAlg (6g) was dispersed in 150ml of distilled water and stirred under 1000 rpm at 80 °C for 30 minutes. The pH of the aqueous solution was adjusted to 9 using ammonia. The aqueous solution was left to cool to 60 °C in the water bath. Monomer aqueous solution composed of predetermined mass of AA and AM with 0.1 wt.% of NMBA were prepared separately and slowly added to sodium alginate aqueous solution. 1g of APS was introduced into the aqueous solution to initiate the polymerization reaction. The solution was left stirring under 1000 rpm at 60 °C for 90 minutes to complete polymerization reaction.

After the polymerization, the hydrogel was dropped through a separating funnel into a beaker with 2 M concentration of calcium chloride solution. The hydrogel beads were dried in the oven at 60 °C to a constant mass.

2.3. Fourier Transform Infrared Spectroscopy (FTIR)

FTIR spectra of the pure NaAlg and AM were recorded using a Perkin Elmer, Fourier Infrared Spectrometer, model Spectrum RX1 within the wavenumber of 4000-400 cm^{-1} . Each sample was scanned for four times by using KBr pellet with the thickness around 0.30mm. AA and grafted copolymers were examined using Attenuated Total Reflectance (ATR) method within the same wavenumber.

2.4. Thermogravimetric Analysis (TGA)

Thermal decomposition temperature and weight loss of pure NaAlg powder and its copolymers were determined using Mettler Toledo TGA analyzer, model SDTA851[°]. Approximately 10 mg of samples were heated from ambient temperature to 550 °C at a heating rate of 10 °C/min under nitrogen purge. The add-on percentage and grafting efficiency were also calculated from TGA data.

2.5. Differential Scanning Calorimetry (DSC) Measurements

The glass-transition temperature (T_g) and melting temperature (T_m) of the pure NaAlg powder and its copolymer beads were determined using Mettler Toledo differential scanning calorimeter, model DSC823[°]. Approximately 10 mg of samples were sealed in a standard 40 μL aluminium crucible and analyzed under min 99.9995% purity of nitrogen purge at a flow rate of 10 ml/min. The temperature range investigated was from ambient temperature to 300 °C at a heating rate of 10 °C/min.

2.6. Surface Morphology of the Copolymer

The surface morphology of the copolymers beads was investigated using the field emission scanning electron microscopy (FESEM), model JOEL, JSM 7601F, Japan.

2.7. Measurement of Water Absorbency

5 samples of each copolymer beads were immersed in excess distilled water (500ml) at room temperature for 5 hours. The swollen sample was then separated from unabsorbed water by filtering through a 100-mesh screen. The water absorbency of the superabsorbent polymer, Q_{eq} , was calculated using Equation 1.

$$Q_{eq} = \frac{m_2 - m_1}{m_1} \quad (1)$$

where, m_1 and m_2 are the mass of the dry samples and the swollen samples, respectively. Q_{eq} is calculated as grams of water per gram of sample.

2.8. Biodegradability by Soil Burial Test

Soil burial test to evaluate the superabsorbent polymer biodegradation was conducted for 90 days. Polymer beads were wrapped with stainless steel wire mesh (325#) in order to minimize the loss of the polymer fragments during burial process. Each polymer bead was buried approximately 5cm beneath the surface of the soil.

Approximately 0.1g of the polymer bead was used in the test. The polymer beads were dug out from soil at different time intervals (10, 20, 30, 50, 70 and 90 days). The beads were washed to remove planktonic microorganism and all the debris and then put in an oven at 60°C overnight. The weight of dried polymer beads was taken.

Weight loss was determined using Equation 2:

$$WL\% = \frac{m_0 - m_t}{m_0} \quad (2)$$

where, $WL\%$ is weight loss in percentage, m_0 is the initial mass and m_t is the final mass. An average of three measurements was taken for each copolymer composition [17].

3. RESULTS AND DISCUSSIONS

3.1. FTIR Analysis

Grafting of AA and AM onto NaAlg backbone and the formation of interpenetrating network as shown in schematic 1. The formation of copolymers was confirmed by FTIR. FTIR spectra of the pure sodium alginate, AA, AM and the grafted copolymer beads were analyzed and presented in Figure 1 and 2 respectively. Pure sodium alginate powder shows -OH stretching absorption peak at 3303 cm^{-1} , -COO- asymmetric stretching at 1632 cm^{-1} and -COO- symmetric stretching peak at 1414 cm^{-1} . The absorption peak at 3180 cm^{-1} for AM indicates -NH stretching. The -OH stretching in AA is represented by the absorption peak from 2500 cm^{-1} - 3000 cm^{-1} .



As can be seen in Figure 1 and 2, the peak region at 1000- 985 cm^{-1} attributed to C-H of the ring on NaAlg still exists, suggesting the NaAlg ring was not opened in the reaction [18]. The peak at 1632 cm^{-1} which represents the carbonyl group in NaAlg is shifted to the higher wave number in the grafted copolymer beads spectra, further indicating the grafting on AA and AM onto the NaAlg backbone. However, it is noteworthy that this peak is shifted more towards the wave number of C=O stretching of amide bands at 1651 cm^{-1} compared to C=O stretching of carbonyl group 1634 cm^{-1} as shown in Figure 1. This may be due to better grafting efficiency of AM compared to AA to the NaAlg backbone. However further investigation need to be carried out to confirm it.

When the copolymers were dropped to calcium chloride solution, beads were formed instantaneously by electrostatic interaction between negatively charged NaAlg and positively charged Ca^{2+} . The crosslinking process with

Ca²⁺ caused an obvious shift of symmetric -COO- stretching bands from 1414cm⁻¹ to higher wavenumber, indicating the formation of ionic bonding between Ca²⁺ and -COO⁻ of NaAlg [19]. The peaks at 1430 – 1435 cm⁻¹ show the Ca²⁺ is crosslinked with the copolymer samples.

3.2. Thermogravimetric Analysis (TGA)

Thermogravimetric analysis (TGA) was conducted to examine the effect of AA and AM composition on the thermal decomposition of the NaAlg copolymers. As evident from the TG and DTG curves of NaAlg and copolymers in Figure 3 and 4 respectively, NaAlg underwent two-step decomposition when heated up to 550 °C, meanwhile all the copolymers underwent four-step decomposition. All the T_{onset}, T_{max}, mass loss and residue for copolymers are summarized in Table 2.

Mass loss of pure NaAlg starts at 55 °C. This decomposition stage is due to removal of moisture and surface bound water from NaAlg. As the composition of AM increases, T_{onset 1}, T_{onset 2}, T_{onset 3}, T_{max 1}, T_{max 2} and T_{max 3} increase. Percentage of mass loss at T_{max 1} and T_{max 2}, which is due to removal of moisture and surface bound water, decreased as the AM concentration increased. This is because compared to AA, AM is non ionic and absorb less water, thus the moisture content is less.

The third decomposition step observed in the copolymers is due to the decomposition of carboxyl group of AA and degradation of AM. The mass loss at this step increases as the concentration of AM increases. T_{max 3} increases from 302.58 °C to 400 °C as the concentration of AM increases. This is due to the formation of imide group by the cyclization of amide group as reported in previous studies [20].

The fourth decomposition step is due to the complex decomposition of NaAlg backbone including dehydration of the saccharide rings, depolymerization with the formation of water, carbon dioxide and methane. T_{onset 4} and T_{max 4} increase slightly as the concentration of AM increases [21].

The mass loss data from TGA can also be used to calculate add-on percentage and grafting efficiency using equations 3 and 4 respectively [22]. The results are also included in Table 2.

$$\text{Add on percentage} = \frac{\text{Weight loss of step [3]}}{\text{Weight loss of step [2,3,4]}} \times 100\% \quad (3)$$

$$\text{Grafting efficiency} = \frac{\text{Weight loss of step [3]}}{\text{Weight loss of [2,4]}} \times 100\% \quad (4)$$

Grafting efficiency increases as the AM concentration increases, and the increment of grafting efficiency increases the thermal stability.

3.3. Differential Scanning Calorimetry (DSC)

Differential scanning calorimetry (DSC) results for pure NaAlg and its copolymers are shown in Figure 5 and the transition temperature values are summarized in Table 3. The DSC traces of sodium alginate exhibit an endothermic at 77.50 °C. The endothermic peak represents T_g (glass transition temperature) for NaAlg, whereas, the exothermic peak are due to decomposition of NaAlg at temperature 248.24 °C. Many other literatures also support this finding. For example, Gao *et al.* (2009) also recorded an exothermic peak at temperature around 250°C for sodium alginate [23]. Moreover,

according to literature study in Ca^{2+} crosslink beads, the decomposition peak was not observed due to the formation of the structure of “egg box” with calcium ions [24]. DSC results indicate that pure NaAlg is semi-crystalline.

All the copolymers exhibit two endothermic peaks; T_g and T_m (melting temperature). The exothermic peak diminished, suggesting improvement of the decomposition temperature for NaAlg copolymers. This improvement might be due to crosslink network formation. Existence of T_m indicates the formation of crystalline region in the copolymers due to hydrogen bonding.

The values of T_g and T_m for each copolymer are influenced by the crosslink network formation and the strength of hydrogen bonding. Different types of hydrogen bonding can occur in all these copolymers due to different concentration of AA and AM. Each of this hydrogen bonds exhibit different strength. Sample C exhibit the highest T_m value, due to the

$\text{O}-\text{H}\cdots\text{N}$ type of hydrogen bond formation when the concentration of AA and AM are almost similar. The T_m value increases from sample A to B, as the possibility for the formation of $\text{O}-\text{H}\cdots\text{N}$ type of hydrogen bond increase as the concentration of AM increases. However, for samples D and E, the T_m value is lower than sample C when the concentration of AM exceeds 50%, more $\text{N}-\text{H}\cdots\text{N}$ type of hydrogen bond will be formed and these bonds are relatively weak compared to $\text{O}-\text{H}\cdots\text{N}$ bonds [25].

In contrast, the T_g value increases proportionally as the concentration of AM in the copolymers increases. AA exhibit an ionic characteristic, whereas AM has non-ionic characteristic. Thus, the copolymers with higher AA will be acidic, while, the copolymer with higher concentration of AM will be more neutral. Previous research shows that neutralized copolymers can be crosslinked much faster than non-neutralized ones, as the initiator and crosslinking agent are activated much faster in neutralized condition [26]. Hence, in the copolymers with high concentration of AM, more crosslinks can be formed in the reaction.

3.4. Morphological Analysis

The micrograph of the superabsorbent polymer beads with different ratio of AA and AM were shown in Figure 6 respectively. It can be observed that all the polymer beads present an undulant and coarse surface, facilitating the permeation of water into polymeric network [27].

The FESEM micrographs show that with increasing concentration of AM, fewer cracks was observed and voids on the surface had been reduced. A more tight/compact surface can be observed with higher concentration of AM as shown by SEM micrographs for copolymers D and E. This is due to AM has higher hydrogen bond strength which makes the surface more compact and exhibit less cracks if compared to copolymers with higher ratio of AA. Copolymer A exhibits the most voids and cracks. As a result, it causes the superabsorbent polymer A having weakest gels strength and strong water absorbency. This will be discussed further in subsection 3.5.

3.5. Water Absorption

Figure 7 shows the effect of various concentration of AA and AM on water absorbency of the copolymer beads. The results indicate that the gel strength for copolymer A is the weakest as the beads start to dissolve in water after 1.5

hours. As the concentration of AM increases, the water absorbency decreases.

AM is a non-ionic monomer, meanwhile AA is an ionic monomer which holds better water adsorption capability in water. The $-\text{COOH}$ group in AA has a better hydrophilic ability than $-\text{CONH}_2$ group in AM due to its higher number of hydrophilic group, so the swelling is much higher [28-30].

3.6. Biodegradability Test

Biodegradability test result is shown in Figure 8. All the polymer beads with AA and AM can be biodegraded. However, the biodegradability percentage remains constant after 30 days. This is due to the lack of the bacterial activity in the soil sample. The biodegradability of the polymer beads will improve if the beads are buried in plantation area with natural condition.

The biodegradability of the polymer beads may also remains constant after 30 days due to the interpenetrating network formation among the copolymer chains. This crosslinked copolymer chains will not biodegrade easily. Moreover the Ca^{2+} layer around the copolymers will also reduce biodegradation of the superabsorbent polymers. Ca^{2+} acts as a protective layer on the surface of the superabsorbent polymers and thus prevents the penetration of microorganism to attack the polymer chains.

From the Figure 8, biodegradability of the polymer beads is faster when the concentration of AM increases. AM acts as soil conditioner which can increase the soil tilt, aeration, and porosity and reduce compaction, dustiness and water run-off and these factors might accelerate degradation in beads with higher concentration of AM.

4.0. CONCLUSIONS

A new multifunctional superabsorbent copolymer with biodegradable properties was successfully prepared by grafting AA and AM on the NaAlg backbone and crosslinking with NMBA. This is confirmed by FTIR result which assures that there is a grafting copolymerisation reaction. The water absorbency was influenced by the ionic and non-ionic nature of AA and AM. As the AM concentration increases, the thermal stability and biodegradability increases whereas the water absorbency decreases. Less cracks and voids were observed on the surface of the polymer beads as the AM concentration increases. This observation is in agreement with the reduction of water absorbency as the concentration of AM increases.

5.0. ACKNOWLEDGEMENTS

The authors gratefully acknowledge the support of Universiti Tunku Abdul Rahman (UTAR) research grant, IPSR/RMC/UTARRF/C1-11/.

6.0. REFERENCES

1. K.L. Baker, S. Langenhede, G. W. Nicol, D. Ricketts, K. Killham, C. D. Campbell, and I.P. James, *Soil Biol. Biochem.* **41**, 2292-2298 (2009).
2. L. Cosgrove, P. L. McGeechan, G. D. Robson, and P. S. Handley, *Appl. Environ. Microbiol.* **73**, 5871-5824 (2007).
3. US Department of Agriculture, US Patent 3,981,100, (1961).

4. J. Zhang, and A. Wang, *React. Funct. Polym.* **67**, 737-745 (2007).
5. Z. B. Chen, M. Z. Liu, and S. M. Ma, *React. Funct. Polym.* **62**, 85-92(2005)
6. K. Nagasuna, N. Suminaga, K. Kimura and T. Shimonura, *Jpn. Patent* 126, 234(1989).
7. J. Zhang, Q. Wang, and A. Wang, *Carbohydr. polym.* **68**, 367-374 (2007).
8. F. Santiago, A. E. Mucientes, M. Osorio, and C. Rivera, *Europ. Polym. Jnl.* **43**, 1-9 (2007).
9. W. F. Lee, and L. G. Yang, *J. Appl. Polym. Sci.* **102**, 927-934 (2006)
10. J. Liu, Q. Wang, and A. Wang, *Carbohydr. polym.* **70**, 166-173 (2007).
11. S. Kiatkamjornwong, K. Mongkolsawat, and M. Sonsuk, *Polymer* **43**, 3915-3924 (2002).
12. S. Kiatkamjornwong, K. Mongkolsawat, and M. Sonsuk, *Polymer* **43**, 3915-3924 (2002).
13. S. Farag, and E.I. Al-Afaleq, *Carbohydr. Polym.* **48**, 1-5 (2002).
14. G.R. Mahdavinia, A. Pourjavadi, H. Hosseinzadeh, and M. J. Zohuriaan, *Europ. Polym. Jnl.* **40**, 1399-1407 (2004).
15. *Handbook of hydrocolloids*, Ed. 2: Alginates by K. I. Draget. In: G. O. Philips, and P. A. Williams (UK: CRC Woodhead Publishing Limited, 2009, pp 380).
16. *Polysaccharides and polyamides in the food industry: properties, production, and patents. Alginates from algae*, Ed. by K. I. Draget, O. Smidsrød, and G. Skjåk-Bræk, G. In: A. Steinbuchel, and S. K. Rhee (Wiley-VCH , Weinheim, 2005, pp 1).
17. C. R. Di Franco, V. P. Cyras and R. A. Ruseckaite, *Polym. Degrad. Stabil.* **86**, 95-103 (2004).
18. L. Yang, X. Ma, and N. Guo, *Carbohydr. Polym.* **85**, 413-418 (2011).
19. Y. M. Xu, C. Y. Zhan, L. H. Fan, L. Wang, and H. Zheng, *Int. Jnl. Pharm.* **336**, 329-337 (2007).
20. Durcilene A. da Silva, Regina C.M. de Paula, and Judith P.A. Feitosa. *Europ. Polym. Jnl.* **43**, 2620-2629 (2007).
21. P. Lanthong, R. Nuisin, and S. Kiatkamjornwong. *Carbohydr. Polym.* **66**, 229-245 (2006).
22. P. Lanthong, R. Nuisin, and S. Kiatkamjornwong. *Carbohydr. Polym.* **66**, 229-245 (2006).
23. C. Gao, M. Liu, J. Chen and X. Zhang. *Polym. Degrad. Stab.* **94**, 1405-1410 (2009).
24. B. Sarmiento, D. Ferreira, F. Veiga and R. António. *Carbohydr. Polym.* **66**, 1-7 (2006).
25. *The Nature of the Hydrogen Bond* by G. Gilli and P. Gilli (Oxford University Press Inc, New York, 2009, pp 222-225).
26. D. Lynda Merlin and D Sivasankar. *Europ. Polym. Jnl.* **45**, 165-170 (2009).
27. Y. Zheng, P. Li, J. Zhang, and A. Wang. *Europ. Polym. Jnl.* **43**, 1691-1698 (2007).
28. A. Pourjavadi, R. Soleyman, and R. G. Barajee, R. G. Starch/Stärke, **60**, 467-475 (2008).
29. E. Karadağ, D. Saraydin, Y. Caldiran, and O. Güven, *Radia. Phys & Chem.* **60**, 203-210 (2001).

30. E. Karadağ, O.B. Üzüm, and D. Saraydin, Mater. Des. **26**, 265-270 (2005).

APPENDICES

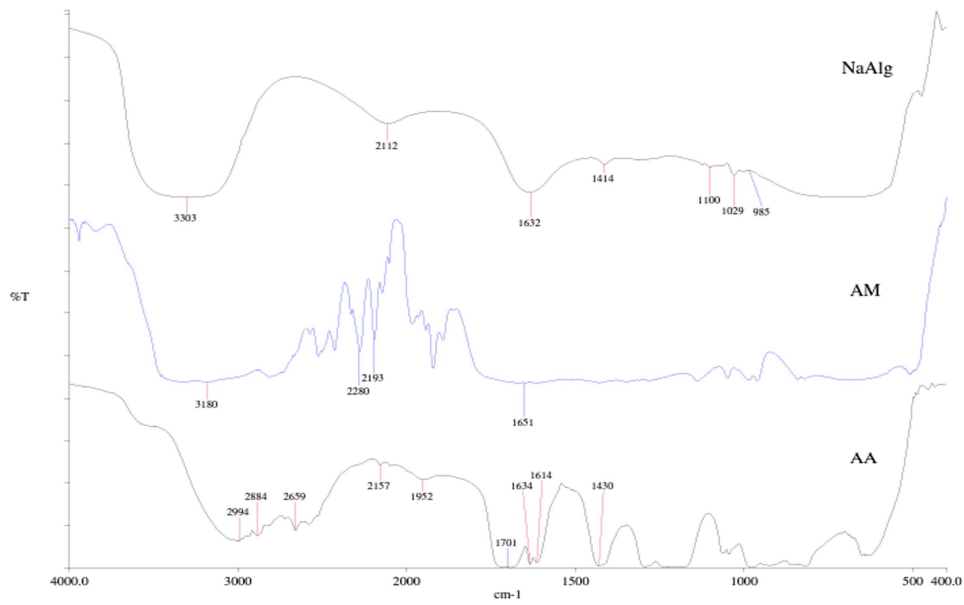


Figure 1: FTIR Spectra of Pure NaAlg, AA and AM

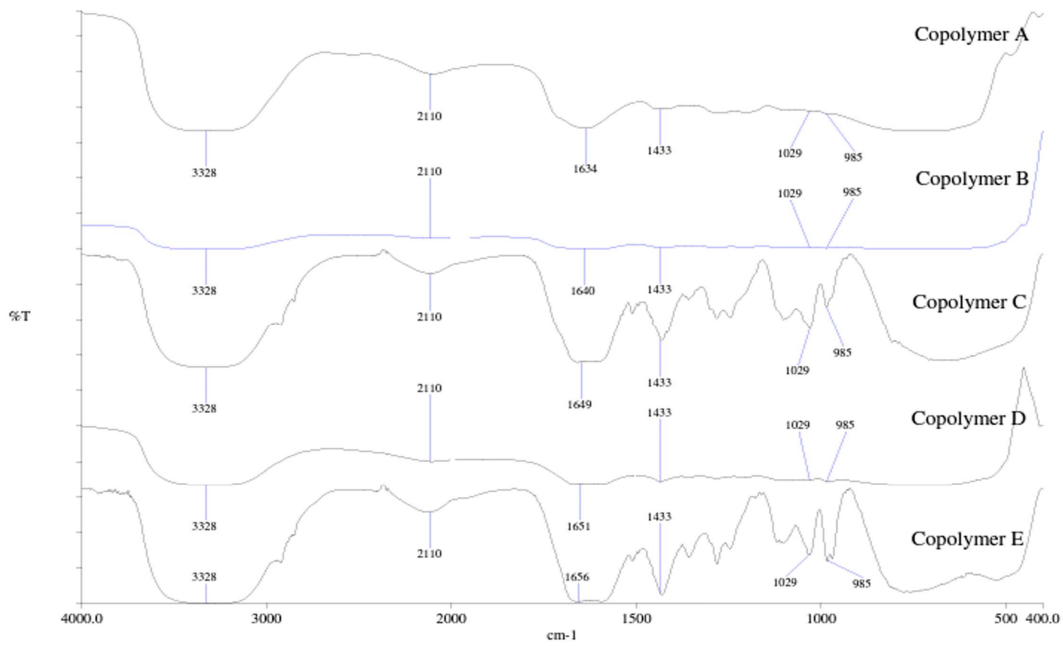


Figure 2: FTIR Spectra of the Grafted Copolymers

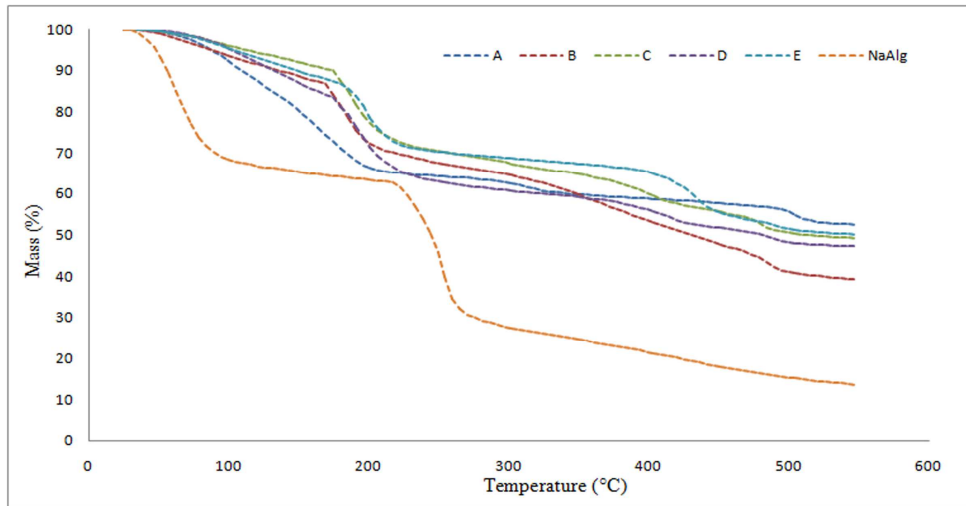


Figure 3: TGA Curves for Pure NaAlg and its Copolymers

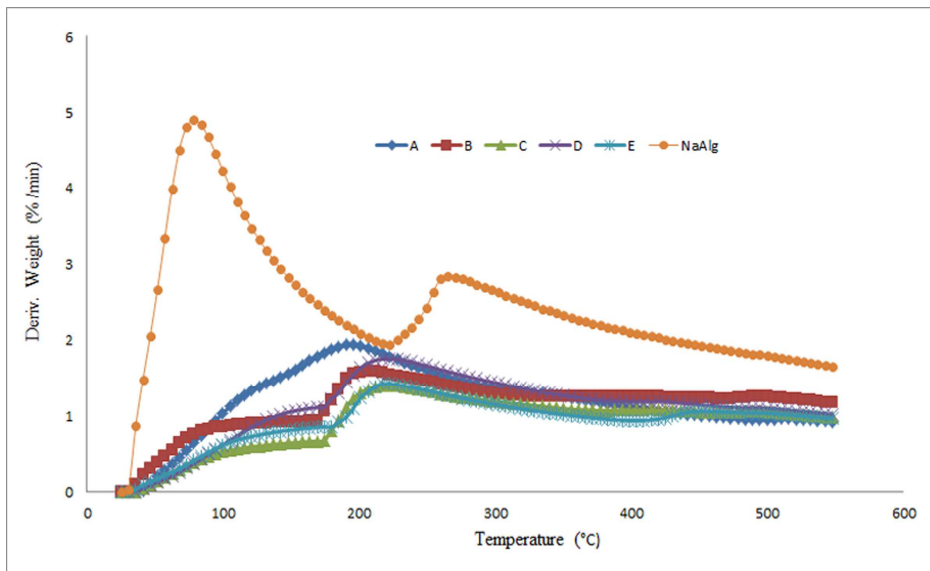


Figure 4: DTG Curves for Pure NaAlg and its Copolymers

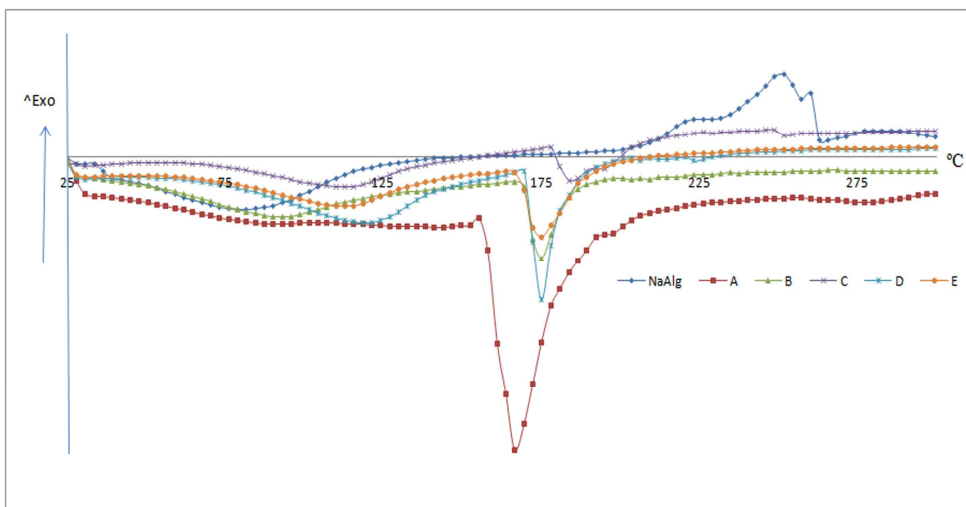


Figure 5: DSC Curves for Pure NaAlg and its Copolymers

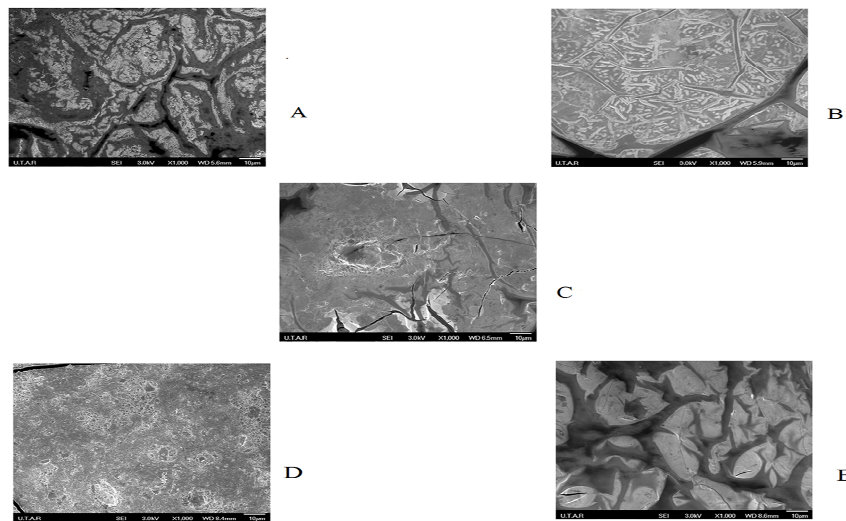


Figure 6: Surface Morphology for Copolymer Beads

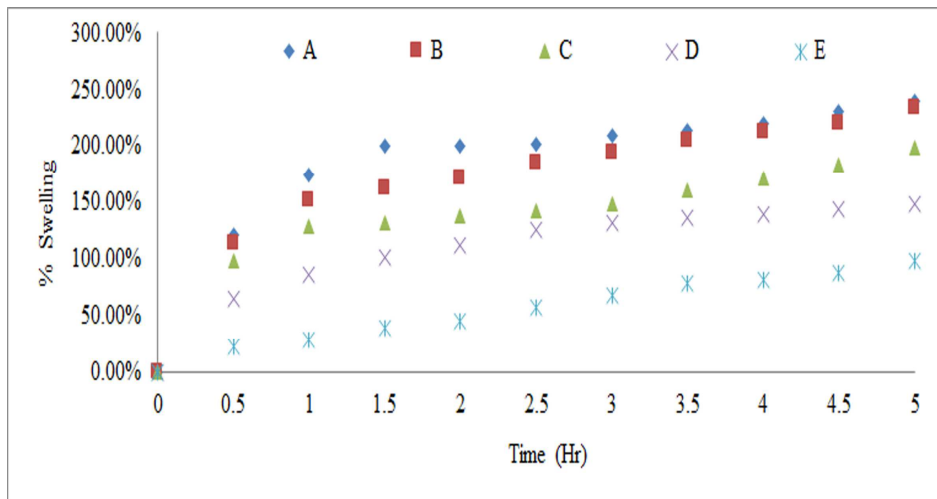


Figure 7: Water Absorbency of Copolymer Beads

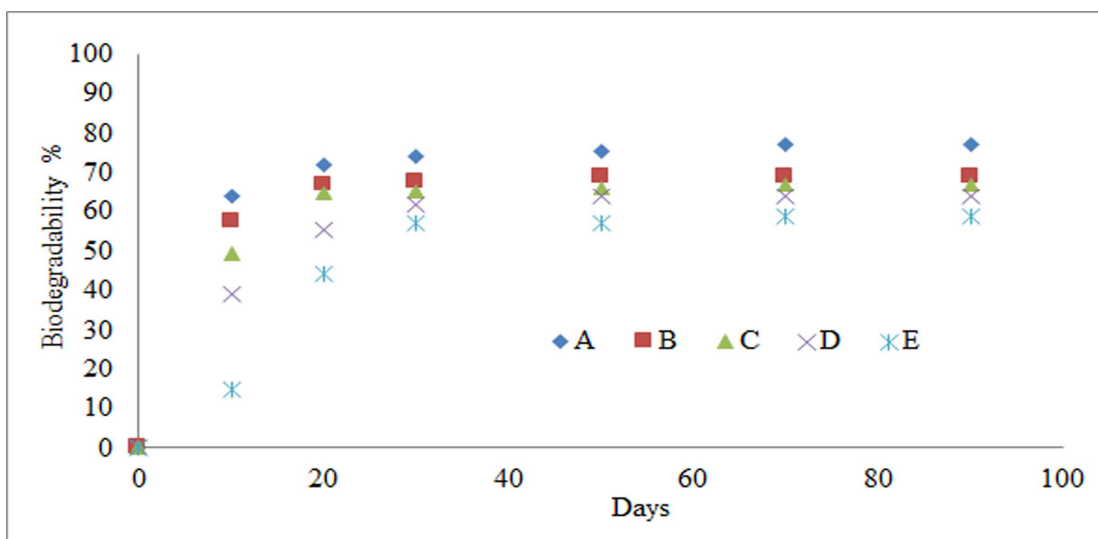


Figure 8: Biodegradability of Copolymer Beads

Table 1: Formulation of Different Weight Ratio of AA and AM

Sample	AA	AM
A	85	15
B	70	30
C	55	45
D	40	60
E	25	75

Table 2: Data Obtained from TGA Analysis

Sample Parameters	NaAlg	A	B	C	D	E
T _{onset 1}	55.28	61.52	65.35	72.72	74.20	79.81
T _{max 1}	79.36	97.99	77.98	88.66	133.53	104.01
Weight loss (%)	20.30	5.47	1.79	1.60	7.78	3.19
T _{onset 2}	236.86	145.98	163.48	172.56	173.81	180.99
T _{max 2}	260.09	182.97	170.95	184.31	185.61	193.64
Weight loss (%)	28.30	13.19	11.46	9.66	9.50	8.45
T _{onset 3}	-	290.85	350.07	362.61	380.55	395.53
T _{max 3}	-	311.93	392.02	395.20	401.98	418.57
Weight loss (%)	-	1.86	1.36	4.83	3.40	7.80
T _{onset 4}	-	460.79	456.81	453.55	458.34	460.98
T _{max 4}	-	491.01	469.53	466.20	472.84	476.56
Weight loss (%)	-	2.10	2.97	2.51	1.93	1.53
Residue (%)	13.50	52.66	45.68	50.38	47.88	50.84
Add on Percentage (%)	-	10.68	12.18%	28.43	30.36%	43.00%
Grafting Efficiency	-	12.18	28.84	39.72	43.59	77.38

Table 3: The T_g and T_m of Pure NaAlg and its Copolymers

Sample	T _g (°C)	T _m (°C)
NaAlg	78	-
A	82	165
B	89	174
C	111	185
D	118	173
E	118	175

